

ENVIRONMENTAL RESEARCH
LETTERS

LETTER

OPEN ACCESS

RECEIVED

21 September 2020

REVISED

12 July 2021

ACCEPTED FOR PUBLICATION

17 September 2021

PUBLISHED

5 October 2021

Original content from
this work may be used
under the terms of the
[Creative Commons
Attribution 4.0 licence](#).

Any further distribution
of this work must
maintain attribution to
the author(s) and the title
of the work, journal
citation and DOI.

Environmental flow requirements largely reshape global surface
water scarcity assessmentXingcai Liu^{1,2,*} , Wenfeng Liu³ , Liu Liu³ , Qiuhong Tang^{2,4} , Junguo Liu⁵ and Hong Yang^{1,6,*}¹ Eawag, Swiss Federal Institute of Aquatic Science and Technology, Ueberlandstrasse 133, CH-8600 Duebendorf, Switzerland² Key Laboratory of Water Cycle and Related Land Surface Processes, Institute of Geographic Sciences and Natural Resources Research, Chinese Academy of Sciences, 11A, Datun Road, Chaoyang District, Beijing, People's Republic of China³ Center for Agricultural Water Research in China, College of Water Resources and Civil Engineering, China Agricultural University, Beijing 100083, People's Republic of China⁴ College of Resources and Environment, University of Chinese Academy of Sciences, Beijing, People's Republic of China⁵ School of Environmental Science and Engineering, Southern University of Science and Technology, Shenzhen 518055, People's Republic of China⁶ Department of Environmental Sciences, MGU, University of Basel, Petersplatz 1, CH-4003 Basel, Switzerland

* Authors to whom any correspondence should be addressed.

E-mail: xingcailiu@igsnr.ac.cn and hong.yang@eawag.ch**Keywords:** water scarcity, environmental flow, hydrological modeling, large-scale, river ecosystemSupplementary material for this article is available [online](#)

Abstract

The inclusion of environmental flow requirements (EFRs) in global water scarcity assessments is essential to obtain a reasonable representation of the water scarcity status. However, at a global scale, the quantification of EFRs is subject to large uncertainties resulting from various methods. So far, it is unclear to what extent the uncertainties in EFRs affect global water scarcity assessments. In this study, we examined the differences between EFR estimation methods and quantified their effects on spatially explicit water scarcity assessments, based on reconstructed global water withdrawal data and naturalized streamflow simulations. The global mean EFRs estimated by different methods ranged from $129 \text{ m}^3 \text{ s}^{-1}$ to $572 \text{ m}^3 \text{ s}^{-1}$. Consequently, with the fulfillment of the EFRs, the area under water scarcity ranged between 8% and 52% of the total global land area, and the affected population ranged between 28% and 60% of the total population. In India and Northern China, 44%–66% and 22%–58% of the country's land area, respectively, is affected by water scarcity; this percentage is higher than that found in other countries. The effects of different EFRs on water scarcity assessment are large in many regions, but relatively small in regions that experience intensive water use due to anthropological activities (such as Northern China and India). Through this study, we have put forth the need for the reconciliation of the estimates of EFRs to produce more reasonable and consistent water scarcity assessments.

1. Introduction

Water scarcity often indicates a shortage of regional water resources and may pose significant threats to food security and the human living environment. Water scarcity has increased over the past decades (Wada *et al* 2011, van Vliet *et al* 2021) and is projected to increase further in the future due to climate change and increasing water demands (Hanasaki *et al* 2013, Schewe *et al* 2014). In addition to human water demands, environmental flow requirements (EFRs)

maintaining the health of river ecosystem is also a key component in water scarcity assessment (Smakhtin *et al* 2004). However, EFRs often conflict with anthropological water use (Richter 2010, Pastor *et al* 2019), and the fulfillment of EFRs may impose large restrictions on the human appropriation of water resources from rivers (Hoekstra and Mekonnen 2012, Hanasaki *et al* 2013, Wada *et al* 2016). EFRs are necessary for the calculation of the Sustainable Development Goal 6.4.2 indicator of water stress (FAO 2019). Notably, EFRs have been considered in recent water

scarcity assessments (Liu *et al* 2016a, 2019); however, varying river regime conditions make the estimation of EFRs both complex and difficult and, therefore, there is a need for further studies, particularly for large-scale assessments (Poff *et al* 2010, Pastor *et al* 2014).

In previous studies, ecologically and hydrologically based approaches have been applied to estimate the EFRs on different scales (Richter *et al* 1997, Arthington *et al* 2006, Acuña *et al* 2020). In large-scale water scarcity assessments, the methods used to estimate EFRs are mostly hydrologically based (Pastor *et al* 2014), mostly relying on the streamflow/runoff (owing to the lack of information on ecological habitat conditions). Some hydrologically based approaches (Tennant 1976, Tessmann 1980) consider the ecological health status of rivers to some extent. However, for simplicity, the global EFRs estimated using these methods often assumed a 'fair to good' ecological status (Jägermeyr *et al* 2017, Pastor *et al* 2019).

In recent literature, EFRs are considered to be an explicit component in water scarcity assessment (Smakhtin *et al* 2004, Wada *et al* 2011, Liu *et al* 2019). This is because the appropriation of streamflow to meet EFRs is necessary to maintain the health of the river ecosystem, which is important for sustainable economic and social development. Therefore, in water scarcity assessment, EFRs should be explicitly represented as an indispensable water user with a high priority, instead of assigning them leftover water resources (after human water use). The EFRs estimated by various methods have been used in water scarcity assessments at river basin and global scales (Pastor *et al* 2014, Theodoropoulos *et al* 2018). The wide range of EFRs used in previous studies has led to large uncertainties and inconsistencies in global water scarcity assessments with respect to their magnitude and spatial distributions. The extent to which different EFR estimates can affect water scarcity assessment is unclear to date. Consequently, it is difficult to determine the affected areas and the number of people suffering from water scarcity and develop appropriate policies to address water challenges.

This study explicitly investigates the uncertainties in surface water scarcity assessments stemming from EFR methods, on a global, regional, and basin scale. The spatial characteristics of the EFRs related to hydroclimatological features were elaborated, and the area and population affected by surface water scarcity were quantified to demonstrate the effects of different estimates of EFRs on the assessments. This study also contributes to improving the understanding of the heterogeneity of the estimates of EFRs on a global scale and the underlying hydrological mechanisms linked to hydroclimate conditions.

2. Methods and data

2.1. Environmental flow requirements (EFRs) estimation

Seven hydrologically based methods (table S1 (available online at stacks.iop.org/ERL/16/104029/mmedia)), namely, the flow duration curve (FDC) method (Q90 and Q50), Tennant method (1976), Tessmann method (1980), variable monthly flow (VMF) method (Pastor *et al* 2014), Q90/Q50 method (Pastor *et al* 2014), and Smakhtin method (2004) were used to estimate EFRs (Liu 2021). Most of these methods are commonly used to determine global EFRs (Jägermeyr *et al* 2017, Pastor *et al* 2019). Two FDC percentages, Q90 (Gopal 2013) and Q50 (median) (USFWS 1981) which are key elements of other methods (e.g. Q90/Q50, Smakhtin) and straightforwardly comparable to others, were considered in this study. Q50 was not used as commonly as Q90 but has been used in recent studies (Belmar *et al* 2011, El-Jabi and Caissie 2019). The Tennant method determines EFRs based on the mean annual flow (MAF). The Tessmann method is a modification of the Tennant method using different proportions of the MAF and mean monthly flow (MMF), considering an intermediate season (Gerten *et al* 2013, Pastor *et al* 2014, Jägermeyr *et al* 2017, Grantham *et al* 2019, Mekonnen and Hoekstra 2020). The VMF method follows the natural variability of river flow and estimates the EFRs monthly in global assessments. The Smakhtin method considers biophysical and environmental flow conditions, defines low flow requirements as Q90, and estimates high-flow requirements based on MAF and Q90. The Q90/Q50 method estimates EFRs as Q90 streamflow for low-flow seasons and Q50 for high-flow seasons (Pastor *et al* 2014). Notably, in the initial application of the Smakhtin method, regulated streamflow is used to calculate the EFRs (Smakhtin *et al* 2004), which is different from other methods. To be consistent in this study, we used the naturalized streamflow for the EFR estimation carried out using all the above methods. EFRs of 10%, 20%, ..., 90% of MAF and Q80, Q70, and Q60 are also applied uniformly worldwide in the water scarcity assessment for sensitivity tests.

Inadequate ecological and management data have made it infeasible to consider the ecological status of individual rivers on a global scale. To ensure the comparability of these methods, a fair ecological condition was assumed for the Tennant, Tessmann, VMF, and Smakhtin methods. The low-flow and high-flow seasons were defined according to the MMF and MAF as per Pastor *et al* (2014); then, all EFR methods were applied on a monthly basis. By definition, the EFRs determined from the FDC based on all the records over the duration of 120 months were found to be constant.

2.2. Water scarcity index (WSI)

The water scarcity index (WSI), defined as the ratio of water withdrawal to water availability, is the most widely used index for global water scarcity assessment (Wada *et al* 2011, Hanasaki *et al* 2013, Liu *et al* 2019). Water withdrawal is the sum of withdrawals of all sectors (including agricultural, industrial, domestic, and livestock sectors). However, human beings cannot use all the available water resources because EFRs must be met to maintain river ecosystem health and for sustainable social and economic development. For this reason, EFRs have been included as a key component in the indicator for assessing the sustainable development goal (SDG) 6.4.2 on water scarcity (FAO 2019). According to the Food and Agriculture Organization (FAO) guidelines, only water in excess of EFRs can be potentially utilized for or allocated to human activities. Hence, water scarcity is defined as the water withdrawal of all sectors divided by the difference between the total renewable freshwater resources and EFRs; water availability is determined as the simulated natural streamflow with the EFRs deducted (Liu *et al* 2019). For comparison, we also calculated the traditional WSI without deducting the EFRs from the available water.

Water scarcity is defined as $WSI > 1$ for the assessments that explicitly consider EFRs, indicating that the available water is insufficient to meet water demands. In previous studies, the threshold for water scarcity was conventionally set as 0.4% or 40% (Alcamo *et al* 2003, Oki 2006, Wada *et al* 2011, Hoekstra and Mekonnen 2012, Hanasaki *et al* 2018), irrespective of whether EFRs are included. However, there is confusion regarding the threshold because the 0.4 threshold without considering EFRs indicates that 40% of the water resources/streamflow can be appropriated for human water use. This implies that 60% of the total water resources is allocated for environmental flow and is not available for any other application. So far, there has been no elaboration for only allowing 40% of water resources for human users and maintaining 60% in the rivers (potentially for environmental use). In our study, EFRs were estimated explicitly, and the quantity was deducted from the water availability. Thus, a WSI greater than 1 indicates that water resources cannot meet the water demands of humans and the natural environment simultaneously. In this case, the conceptual meaning of the threshold of 1 is clear, although the desired threshold can be closely related to societal choices (FAO 2019). However, a threshold of 0.4 is still used for the WSI calculated without the explicit consideration of EFRs. Thus, the water scarcity assessment using threshold 1 can be compared with the traditional water scarcity assessment applied without the explicit consideration of EFRs.

In this study, the water scarcity assessment is presented as multi-year means, based on the monthly WSI at grid cells over the 2001–2010 period. The WSI

values were averaged over 10 years for each month. The area under water scarcity (in percentage; A_{ws}) is the sum of areas of the grid cells with $WSI > 1$ ($WSI > 0.4$ for those without EFR) in specific regions/basins, portrayed as the percentage of total land areas for each month, and is then, averaged over the study period. Like A_{ws} , the population affected by water scarcity (P_{ws}) is the sum of the population within the grid cells with $WSI > 1$ ($WSI > 0.4$ for those without EFR) in specific regions/basins, portrayed as the percentage of the total regional population. Greenland and the grid cells having an annual mean discharge of $< 5 \text{ m}^3 \text{ s}^{-1}$ were excluded from the calculation of A_{ws} , P_{ws} , and the following analysis.

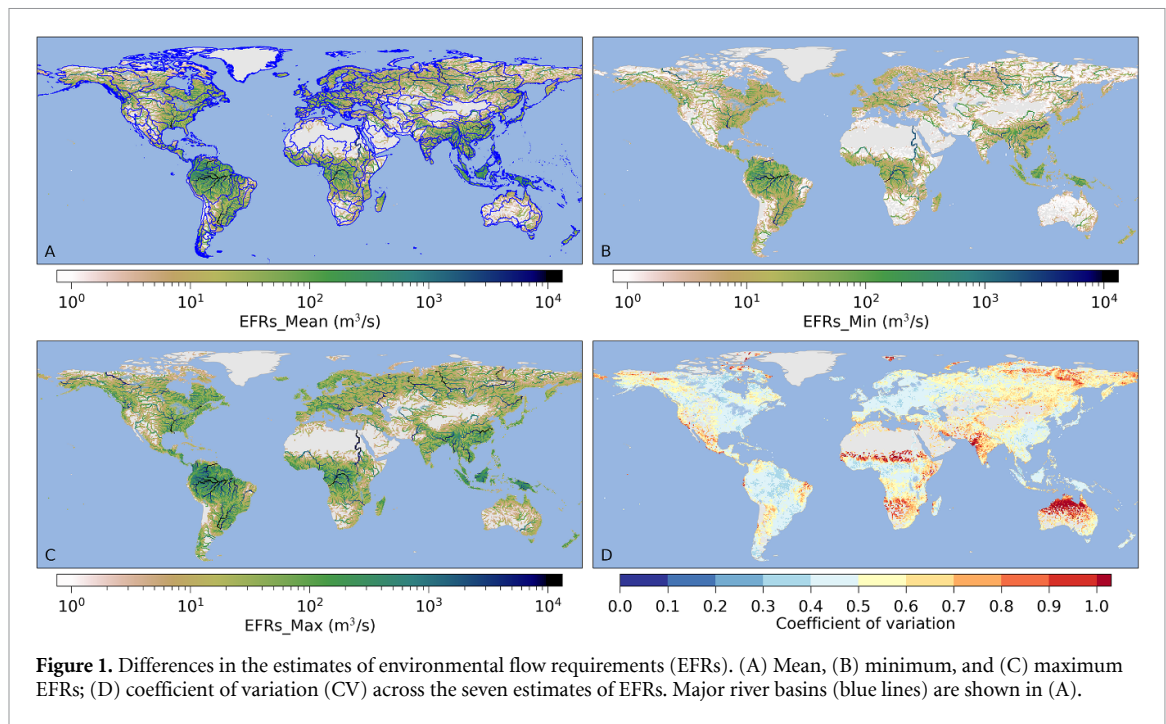
2.3. Streamflow and water withdrawal data

Water availability was determined from the multi-model simulations of the monthly natural streamflow of the NOSOC experiment, that is, without the consideration of human impact (in pristine condition), at a spatial resolution of half-degree. The multi-model simulations were archived in the Inter-Sectoral Impact Model Intercomparison Project (ISIMIP) 2a dataset (Gosling *et al* 2017). Simulations over the 2001–2010 period from six global hydrological models (GHMs) were considered, including DBH (Tang *et al* 2008, Liu *et al* 2016b), H08 (Hanasaki *et al* 2008), LPJmL (Bondeau *et al* 2007, Biemans *et al* 2011), PCR-GLOBWB (Wada *et al* 2014), and WaterGAP (Müller Schmied *et al* 2014). These GHMs were forced by three global meteorological data, namely PGMFD v.2 (Sheffield *et al* 2006), GSWP3 (<http://hydro.iis.u-tokyo.ac.jp/GSWP3/>), and WFDEI (Weedon *et al* 2014) datasets. The global 30 min drainage direction map (DDM30) (Döll and Lehner 2002) was applied to the six GHMs to obtain the river flow. The uncertainty in the streamflow simulations has been documented in previous literature (Liu *et al* 2017, Zhao *et al* 2017) and is not the scope of this study. Thus, monthly streamflow medians were computed from the 18 combinations of individual GHMs and individual forcings at each grid cell to determine the water availability.

For water withdrawal, we used the global water withdrawal data with a spatial resolution of half-degree which was reconstructed based on the data reported by the FAO and the GHM simulations during 1971–2010 (Huang *et al* 2018). In this dataset, the water withdrawal from the FAO AQUASTAT database was used to adjust the global gridded of water withdrawals simulated by four global hydrological models (H08, LPJmL, PCR-GLOBWB, and WaterGAP2) from the ISIMIP2a dataset.

2.4. Regional analysis

Analysis was also performed based on river basins and hot spot regions to examine the impacts of EFRs on water scarcity over regions having different hydroclimatic regimes. Hot spot regions were



identified according to water scarcity conditions and the intensity of water withdrawal (figure S1). A_{ws} and P_{ws} were calculated for each hot spot region and basin and averaged over the period. The mean aridity index (AI, the ratio of total precipitation to potential evapotranspiration) (Trabucco and Zomer 2019) was calculated to represent the climatic conditions in individual river basins. The map of global major basins (figure 1(A)) was obtained from the FAO GeoNetwork (<https://data.apps.fao.org/map/catalog/srv/eng/catalog.search?id=30914%26;currTab=simple#/metadata/7707086d-af3c-41cc-8aa5-323d8609b2d1>, accessed on 2021-7-10).

3. Results

3.1. Differences in the estimated environmental flow requirements (EFRs)

The estimated mean monthly EFRs (figure 1(A)) generally show patterns similar to those of streamflow (figure S1), that is, EFRs are high in wet regions and low in arid regions. Specifically, EFRs are generally large in the Amazon River, Congo River, Yangtze River, and several rivers in tropical regions and high latitudes. In our study, the minimum (figure 1(B)) and maximum (figure 1(C)) EFRs showed similar spatial patterns to the mean EFRs. The coefficient of variation (CV) indicates the relative differences between these EFRs across the world, which is larger than 0.5 in more than 70% of the global land areas and ~ 1 in most arid regions (figure 1(D)). The mean monthly EFRs showed significant differences among the EFR methods in many regions (see figures S2 and S3 in the supplementary information (SI) for the EFRs for high, low, and intermediate flow).

The estimated global mean EFRs by different methods were quite distinct from each other in terms of their mean values and seasonal cycles (figure 2(A)). The Q50 and Q90 EFRs were constant in all months because they were determined from the FDC estimated for the entire period. The EFRs estimated using the Q90/Q50, Tessmann, VME, and Tennant methods showed similar seasonal patterns, with larger values from March to July; the global mean EFRs estimated using the Smakhtin method were larger from May to November. Global mean EFRs calculated using Q50 were the largest ($428 \text{ m}^3 \text{ s}^{-1}$), followed by those calculated using Q90/Q50 ($308 \text{ m}^3 \text{ s}^{-1}$). The Tennant method provided the smallest global mean EFRs ($96 \text{ m}^3 \text{ s}^{-1}$), followed by the VMF EFR ($174 \text{ m}^3 \text{ s}^{-1}$). The Tessmann, Smakhtin, and Q90 methods had relatively similar global mean EFRs of $243 \text{ m}^3 \text{ s}^{-1}$, $221 \text{ m}^3 \text{ s}^{-1}$, and $213 \text{ m}^3 \text{ s}^{-1}$, respectively.

The basin EFRs estimated using Q50 were always the largest, while the smallest basin EFRs are often obtained using the Smakhtin, Q90, and Tennant methods. The EFRs estimated using the VMF method often lay between those estimated using all the methods. The basin EFRs generally increased with the AI (figure 2(B)), that is, the EFRs of wetter basins were larger than those of the drier ones. This trend, estimated from the EFRs obtained using all the methods, is more significant for dry basins ($\text{AI} < 0.65$) than wet basins ($\text{AI} \geq 0.65$).

3.2. Water scarcity assessments with and without the consideration of environmental flow requirements (EFRs)

The mean monthly WSIs with and without the consideration of EFRs over the 2001–2010 period are

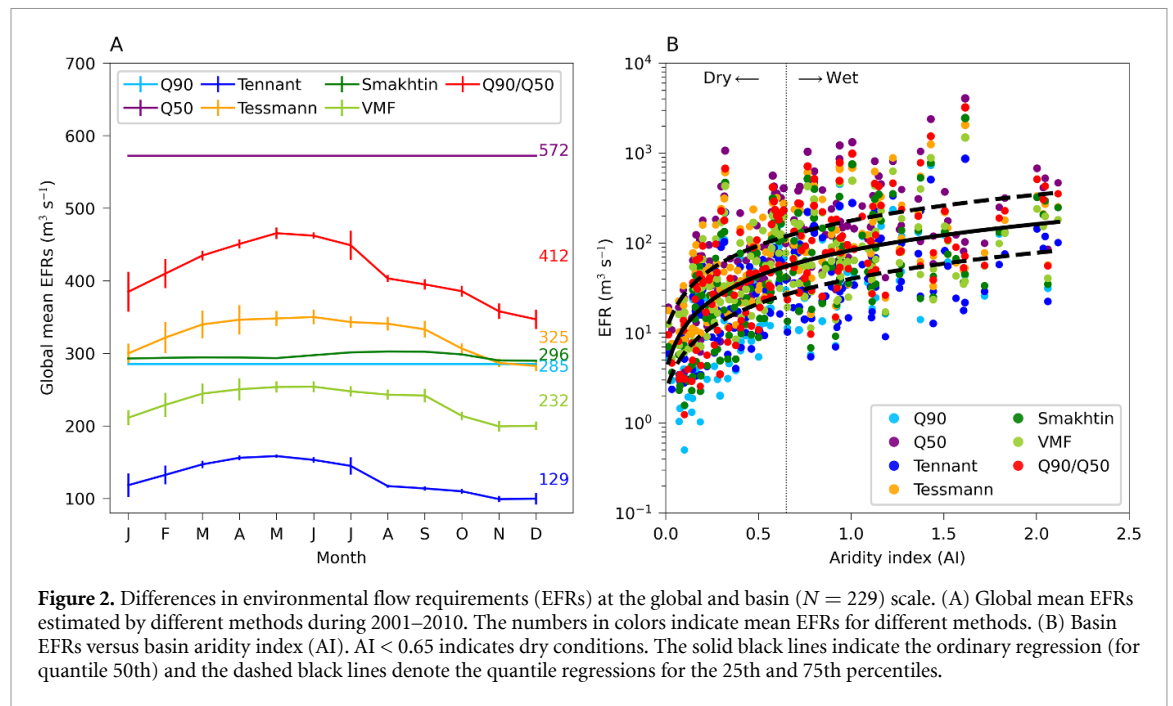


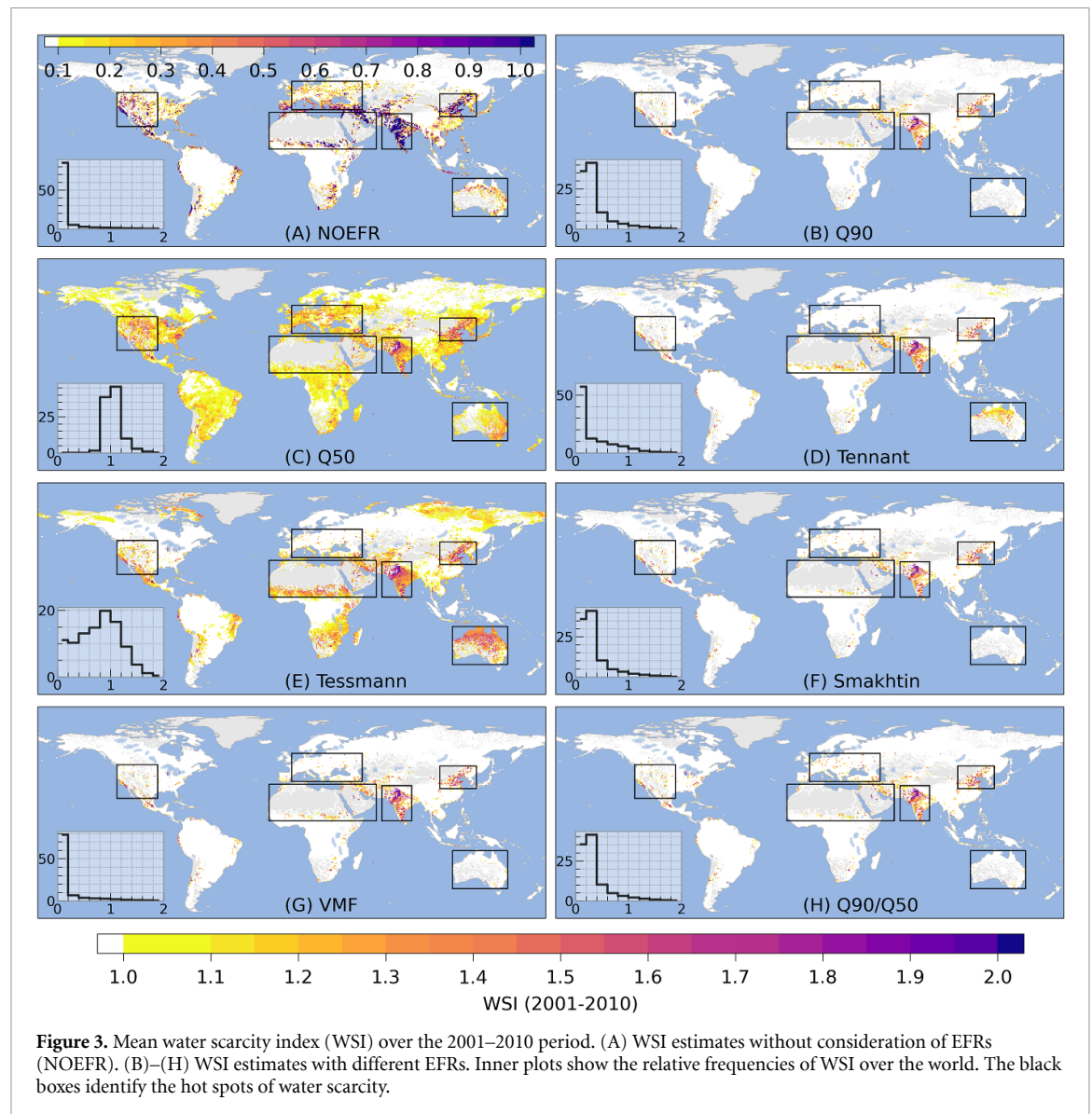
Figure 2. Differences in environmental flow requirements (EFRs) at the global and basin ($N = 229$) scale. (A) Global mean EFRs estimated by different methods during 2001–2010. The numbers in colors indicate mean EFRs for different methods. (B) Basin EFRs versus basin aridity index (AI). AI < 0.65 indicates dry conditions. The solid black lines indicate the ordinary regression (for quantile 50th) and the dashed black lines denote the quantile regressions for the 25th and 75th percentiles.

shown in figure 3. Water scarcity indicated by the WSI without EFRs was mostly found in Central Asia, South Asia, East Asia, Western North America, and North Africa (figure 3(A)). In our study, the extent of water scarcity estimated was generally consistent with previous studies (Oki 2006, Wada *et al* 2011), except for larger areas found in North Africa and Central Asia. Compared to the traditional WSI, a larger extent of water scarcity was indicated by the Q50 and Tessmann WSIs, while less water scarcity was indicated by other WSIs with EFRs. Notably, WSIs with EFRs showed distinct spatial patterns across different EFR methods. The WSI with Q50 EFRs appears to be the largest, showing WSI values >1 in more than half of global land areas covering both humid and arid regions (figure 3(C)), and most WSI values range between 0.8 and 1.2 (see the inner plot). Although the EFRs estimated by the Tessmann method showed spatial patterns similar to those of Q50, the WSI with Tessmann EFRs shows a smaller extent of water scarcity compared to the WSI with Q50 EFRs. The WSI values with Tessmann EFRs showed a wider histogram than Q50, and high values were largely found in arid regions (figure 3(F)). WSIs calculated using Q90 (figure 3(B)), Smakhtin (figure 3(F)), and Q90/Q50 (figure 3(I)) EFRs were similar in terms of their spatial patterns and relative frequencies. The relative frequency of the WSI using Tennant EFRs was different from the WSI obtained using the EFRs by Q90, Smakhtin, and Q90/Q50; specifically, the Tennant WSI showed more values less than 0.2 and more values greater than 1 (figure 3(D)). The WSIs estimated using VMF EFRs (figure 3(G)) showed similar spatial patterns and relative frequency distributions compared to the WSIs estimated without EFRs (figure 3(A)).

The A_{ws} showed evident zonal patterns, indicated by large variations across latitudes, for all the WSI estimations (figure 4(A)). The A_{ws} was generally the largest between latitudes 10° N and 45° N , home to a large human population, followed by the zones between 40° S and 20° S . Relatively large percentages were also found at high latitudes, for example, between 60° S and 40° S and between 70° N and 80° N , for the WSIs estimated using Tessmann and Q50 EFRs.

The seasonality of global A_{ws} showed distinct differences across the WSIs (figure 4(B)). The A_{ws} showed little variation over months for the WSIs calculated using VMF and Tennant EFRs and the WSI calculated without EFRs. The WSIs calculated using Q50 and Tessmann EFRs indicated larger A_{ws} values from October to January (compared to other months). The WSIs calculated using Q90, Smakhtin, and Q90/Q50 EFRs showed almost the same A_{ws} values, with relatively large A_{ws} from January to March and August to September. The WSI calculated without EFR estimated the global A_{ws} as 16% on average. The A_{ws} indicated by the WSI calculated using Q50 EFRs was the largest (54%), followed that calculated using Tessmann EFRs (45%). The WSIs calculated using Q90, Q90/Q50, Tennant, and Smakhtin EFRs indicated A_{ws} values of 21%–23%, and the WSI calculated using VMF EFRs indicated the same global A_{ws} (16%) as that calculated without EFRs.

The seasonality of A_{ws} showed regional differences, as well as differences between the EFR methods, as demonstrated by the six hot spot regions (figure 4(B)). In America and Europe (in North Africa, Arabia, and Australia), the A_{ws} values indicated by the WSIs calculated using Q50 EFRs were larger (smaller) than those calculated using Tessmann

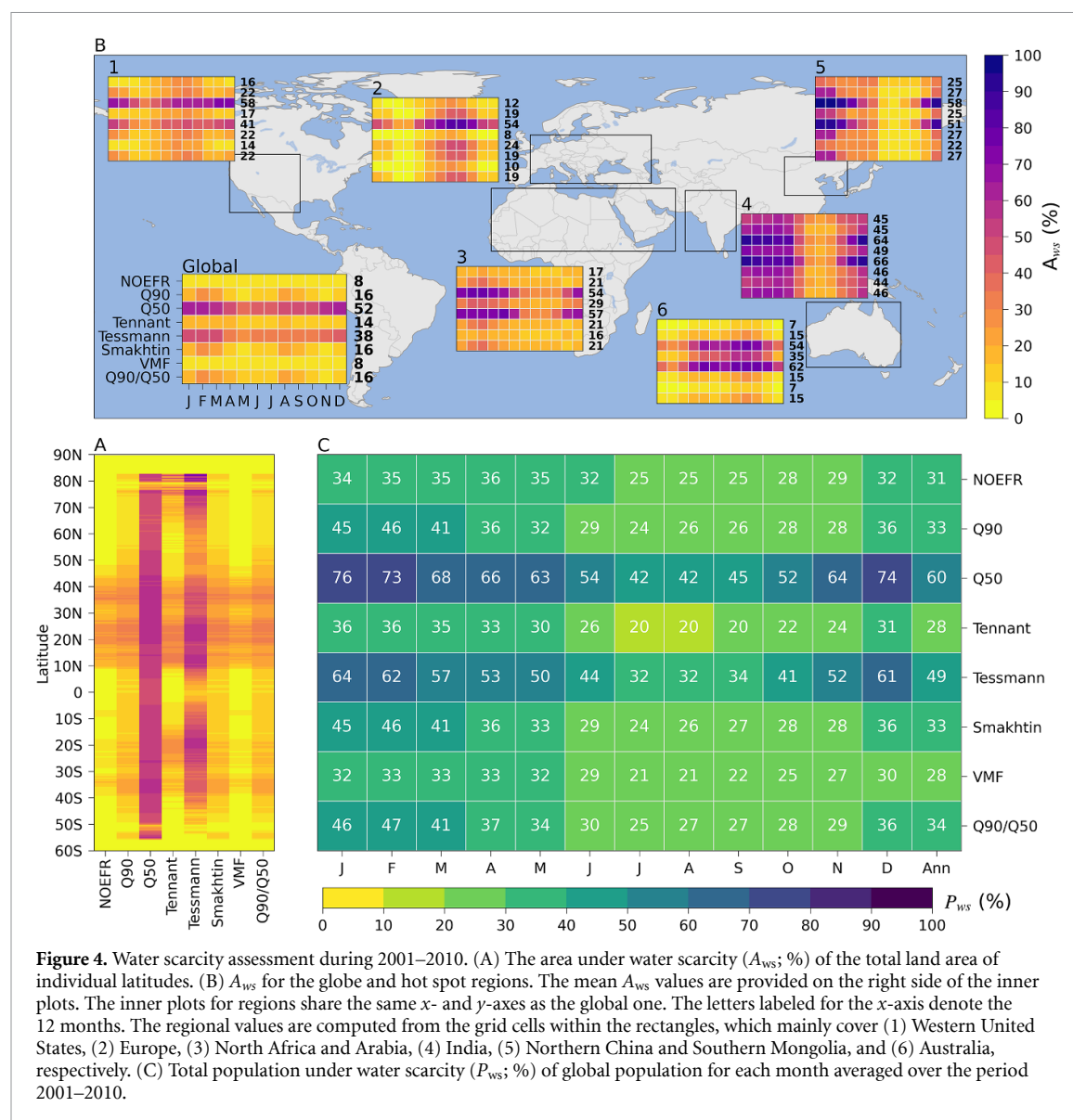


EFRs; however, the A_{ws} values for Northern China and India were similar. The A_{ws} calculated using Q90 EFRs was slightly lower than that calculated using Q90/Q50 EFRs, and both were very close to the A_{ws} values calculated using Smakhtin EFRs. The A_{ws} calculated using Tennant EFRs was small in Europe (9%), while the A_{ws} calculated using VMF EFRs was relatively small in all regions. A_w calculated without EFR was often large in arid/semiarid regions, such as North Africa, Arabia, and Northern China.

The WSIs without EFRs provided P_{ws} estimations of 34% of the global population, while the WSIs with EFRs indicated that 30%–60% of the global population is experiencing water scarcity, on average (figure 4(C)). The WSIs with Q50 (61%) and Tessmann (50%) EFRs indicated the largest population experiencing water scarcity, while the WSIs with Q90, Tennant, Smakhtin, VMF, and Q90/Q50 indicated 35%, 30%, 35%, 31%, and 36% of the global population experiencing water scarcity,

respectively. Notably, on a global scale, less population experienced water scarcity in boreal summer (July–September) than other seasons.

The impact of the different EFRs on water scarcity assessment in terms of the affected area (A_{ws}) and affected population (P_{ws}) at the basin level (figure 5(A)) showed similar differences to those at the global and regional levels. The A_{ws} and P_{ws} were large (40%–60%) in most basins, indicated by the WSIs calculated using Q50 and Tessmann EFRs, and relatively small for those calculated using Q90, Smakhtin, Tennant, and VMF EFRs. The A_{ws} and P_{ws} were relatively larger in arid basins ($AI < 0.65$) and wet basins ($AI \geq 0.65$). The relationships between the ΔA_{ws} (changes in A_{ws} compared to those without EFRs) and AI are distinct for the FDC-based methods (e.g. Q90) and MAF/MMF-based methods (e.g. Tennant and Tessmann) at the basin level (figure 5(B)). The ΔA_{ws} increased with AI when the Q90, Q50, Smakhtin, and Q90/Q50 methods were used and



decreased with the AI when the Tennant and Tessmann methods were used (see also table S2). Water scarcity in terms of affected areas and population increased with EFRs, with respect to the proportions of the MAF (figure 5(C)) and quantiles (figure 5(D)). In particular, the A_{ws} and P_{ws} values estimated by individual FDC-based methods showed less differences between basins than individual MAF-based methods, and they were more distinct between the quantiles than the MAF, even in wet basins.

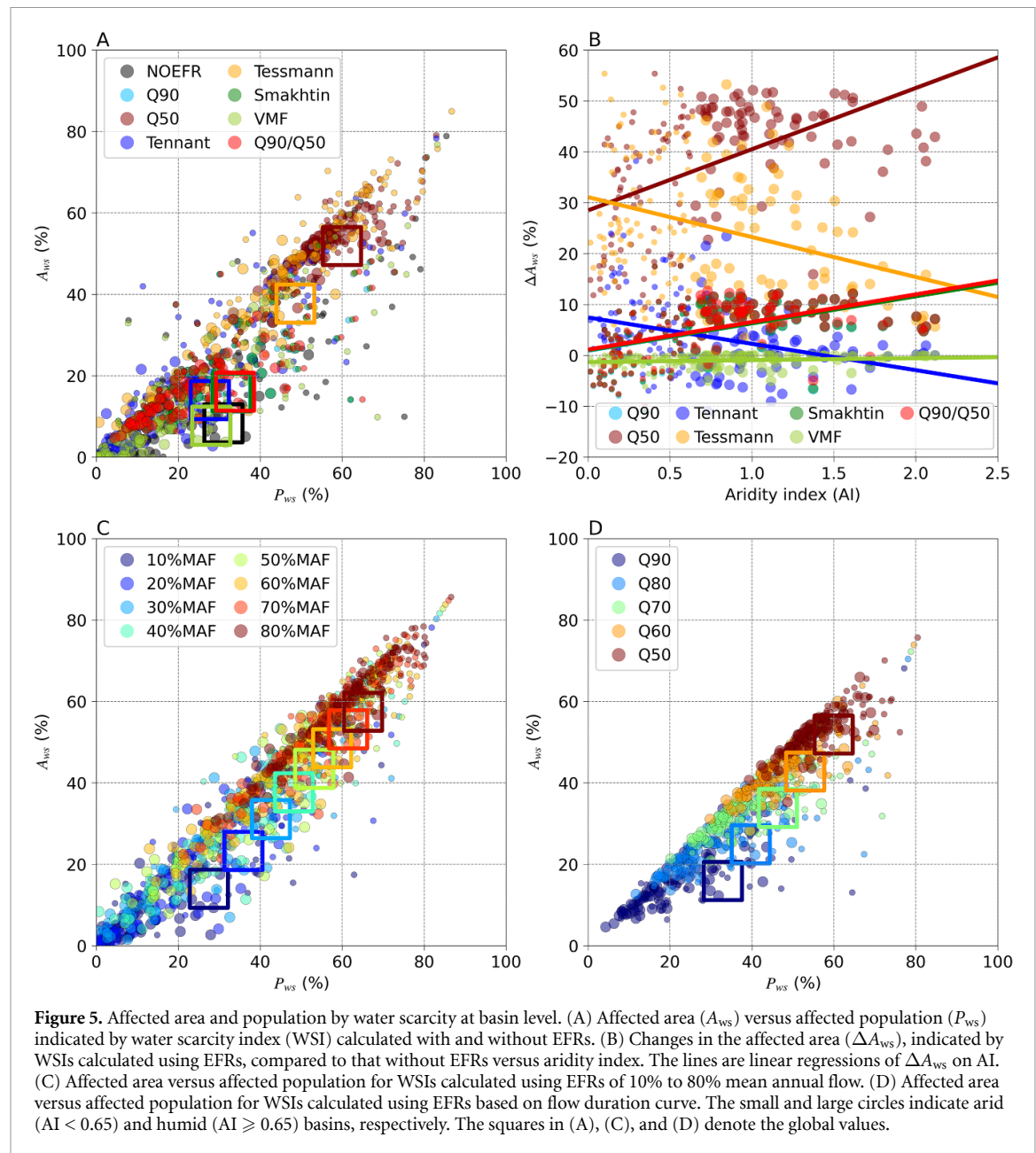
4. Discussion

4.1. Uncertainties in the estimates of environmental flow requirements (EFRs)

The EFRs are subject to considerable uncertainty, as indicated by the large differences in the results obtained using the different methods. The differences between the EFRs in terms of CV showed distinct spatial and seasonal patterns; in particular, they were larger in dry regions (compared to wet regions)

(figure 1). This pattern resembled the temporal variation in the streamflow (figure S1(B)), that is, a high CV of EFRs was found in regions having highly variable monthly streamflow. The CV of the EFRs was most likely associated with streamflow variation, which is a key factor in some EFR methods.

The single ecological status ('fair' condition) across the world may also bring uncertainty into the EFR estimates in regions that expect other ecological conservation goals (Poff *et al* 2010). However, given the difficulties in determining the ecological conditions of rivers worldwide, using a uniform ecological condition across the world would be a practical choice for global assessment. The ecological management classes may be a promising framework for estimating the EFRs that relate to the current or desired condition of a river and are perceived as scenarios of the environmental state of rivers (Sood *et al* 2017, FAO 2019). It considers the ecological condition and management perspectives for both natural (unmodified) and human-disturbed river ecosystems. The



EFR estimates could be more reasonable by setting different classes for regulated and unregulated rivers. Meanwhile, increasing global ecological data (Sayre *et al* 2014, Ghiggi *et al* 2019, Jeliaskov *et al* 2020) will favor global water scarcity assessments with consideration of ecological conditions.

According to the differences in EFRs (figure 2) and their definitions, the EFR methods can be roughly grouped into two types. One type is MAF/MMF-based, for example, Tennant, Tessmann, and VMF. These methods show different levels of EFRs in terms of the absolute values and the proportions of MAF (figures 1 and S5), and the proportions of MAF show little spatial heterogeneity (figure S4). The other group is FDC-based, that is, the Q50, Q90, and Q90/Q50 methods. The EFRs estimated by these methods often largely differ from each other because of the different percentiles used and show large spatial

variability in terms of the proportion of MAF (figure S5). The Smakhtin method uses the information of both Q90 and MAF, but has similar patterns as the Q90 method. We noticed that, for the FDC-based methods (i.e. Q90/Q50 and Smakhtin methods), the ratios of EFRs to MAF calculated in this study were different from the results of Pastor *et al* (2014). This might be because we used the medians of multimodel simulations of natural streamflow, while Pastor *et al* (2014) used the LPJmL simulation only.

4.2. Effects of uncertainties in environmental flow requirements (EFRs) on water scarcity assessment

The large discrepancy between the EFR methods is the major source of uncertainty in the WSI estimates. The uncertainty in terms of the standard deviation (STD) across the WSI estimates with different EFRs (figure S6(A)) is larger than the STD across the WSIs

estimated from the streamflow simulation of individual combinations of GHMs and global meteorological forcing (figure S6(B)). The uncertainty arising from EFRs dominates the uncertainty in the WSI estimates in most areas of the world (figure S6(C)).

The area and population affected by water scarcity showed small differences between the WSIs that used the FDC-based EFR methods, such as Q90, Q90/Q50, and Smakhtin. These methods produced different EFRs (figures 2 and S5), but the area and population experiencing water scarcity showed similar spatial patterns (figure 4). In contrast, the differences between the WSIs with MAF (or MMF)-based EFRs were more significant. The ΔA_{ws} estimated using FDC-based and MAF-based methods showed distinct responses to climate conditions at the basin level (figure 5). This may be because the EFRs estimated by the MAF-based methods accounted for spatially uniform proportions of MAF across regions, irrespective of their climate conditions, while the FDC-based EFRs accounted for different proportions of MAF worldwide (figures S4 and S5). The sensitivity test (figures 5(C) and (D)) showed that water scarcity conditions were more different between FDC-based percentiles than between the proportions of MAF. Compared to each other, the FDC-based methods estimated larger EFRs in wet basins and smaller EFRs in dry basins, whereas the MAF/MMF-based methods estimated smaller EFRs in wet basins and larger EFRs in dry basins.

4.3. Implications for the choice of environmental flow requirements (EFRs) in global water scarcity assessment

EFR is a key component of the indicator for assessing the SDGs on water scarcity (FAO 2019). The large uncertainty in WSIs arising from different EFRs suggests an urgent need to develop a more versatile method or to reconcile the estimates of EFRs to derive a consistent water scarcity assessment across regions and river basins having varied hydrological regimes worldwide. Currently, hydrological methods or desktop approaches using global datasets, such as the methods used in this study, are the most appropriate for a global assessment (FAO 2019). However, there is often no unique EFR method having wide applicability to all hydrological regimes or habitat types (Pastor *et al* 2014). Furthermore, the determination of EFRs could be more complex in the real world, as they are associated with desired conservation goals, water quality, water withdrawals, socioeconomic status, and hydroclimatological conditions (Döll *et al* 2009, Acreman and Arthington 2018). In particular, human intervention, of which the most impacts should be attributed to dams and reservoirs, can alter hydrological regimes, result in significant losses of river connectivity, impair riverine ecosystems worldwide (Grill *et al* 2019); however, they may also regulate streamflow to maintain

the designed EFRs during different seasons. Overall, the methods explicitly addressing seasonality would have a large potential for producing appropriate EFRs because the intra-annual hydrological variation is essential for maintaining river ecosystem health (Richter *et al* 1996), while fixed unique percentages (e.g. Q90 or 60%) seem inappropriate for large-scale assessment (Armstrong and Nislow 2012).

The results of this study can help in the selection of EFR estimation methods by applying the rule of thumb (concerning hydrological regimes) that large EFR estimates are acceptable if they do not cause aggravated water scarcity. In this study, we assumed that larger EFRs would generally favor better conditions of the river ecosystem. However, EFR estimates are often low in arid and semiarid regions, where rivers are often ephemeral and intermittent streams. In these regions, river ecosystems face more serious challenges to maintain their normal conditions and diversity with limited water (Gopal 2003). In this case, it is imperative to address the seasonal variability of the EFRs, which can be inferred from hydrological regimes. Thus, the methods that produce fixed small EFRs (e.g. Q90, see figure 2(B)) may be a practical choice but might not reveal the potential water stress suffered in these regions. Q90/Q50 would be more appropriate than Q90 because the former estimates larger EFRs than the latter and results in a slight aggravation of the water scarcity condition. The Q50 method estimates the largest EFRs, indicating widespread water scarcity, even in humid regions (figure 5). This implies that Q50 may not be suitable for wet regions because it may overstate the water scarcity status during the dry season. In contrast, the Tessmann method could be a good choice for most wet regions because it estimates large EFRs and does not cause significant water scarcity. This may be due to the consideration of the seasonality of natural streamflow in the Tessmann method. The similar impacts on water scarcity calculated using the Q90, Smakhtin, Tennant, and VMF methods suggest that the method that estimates the largest EFRs would be a better choice in wet regions, but the one addressing seasonality would be more appropriate in dry regions. In addition, the Tennant method (MAF-based) is often more suitable for rivers with stable flow regimes, whereas the VMF method (MMF-based) is appropriate for those with larger hydrological variability. This is in line with the findings of Pastor *et al* (2014). These implications would favor future investigations regarding the reconciliation of EFR methods or the design of new methods by taking into account hydrological regimes, as well as ecological conditions, on a global scale.

4.4. Limitations in the estimates of water scarcity index (WSI)

This study focuses on surface water scarcity and estimates the surface water availability from

streamflow. The total water availability might be underestimated in some regions where streamflow, groundwater, desalination water, and rainwater harvesting are available. As the world's largest distributed store of freshwater, groundwater plays a critical role in sustaining ecosystems (Taylor *et al* 2013) and is a major source of water availability in some regions. The interactions between groundwater and climate/surface water are very complex and vary over space (Cuthbert *et al* 2019a); thus, the contributions of groundwater to total water availability could differ significantly across regions. In the regions where the water table is topography-controlled, groundwater is often recharged by precipitation/river flow during wet seasons and, in turn, recharges the river flow during dry seasons. The long-term dynamics of groundwater can be represented by river flow to some degree, but in these regions, the seasonality would not be well captured in the water availability based on naturalized streamflow. In recharge-controlled regions, such as the North China Plain and the southwestern United States, groundwater recharge is more episodic and often dominated by losses from ephemeral flows or intense rainfall/flooding events, with limited interactions between groundwater and streamflow/climate (Cuthbert *et al* 2019a, 2019b). In these regions, water supply significantly relies on groundwater, and thus, neglecting groundwater may underestimate water availability and result in biased WSI estimates. However, it should be noted that high groundwater abstraction and lack of recharge from precipitation/river flow would result in overexploitation or persistent groundwater depletion (Wada *et al* 2010), which would not be sustainable and can lead to chronic severe water scarcity. Overall, the WSI estimated without the consideration of groundwater should be treated with caution in regions having limited interactions between groundwater and streamflow. Thus, incorporating groundwater in future studies related to EFRs and water scarcity assessment is a challenging but important task.

Desalination water, rainwater harvesting, and treated wastewater reuse could also be important sources of water availability in some regions. Desalination water is often used in coastal arid regions. The total desalination water use is estimated to be approximately 1%–4% of the global total water withdrawal (Wada *et al* 2011, Hanasaki *et al* 2016, Gude 2017, van Vliet *et al* 2021). Rainwater harvesting is considered to be an interim or primary water source for domestic use in arid and semiarid areas (Lo and Gould 2015), and the implementation of rainwater harvesting systems is strongly influenced by economic constraints and local regulations (Campisano *et al* 2017). Thus, overlooking the contribution of desalination and rainwater to water availability may introduce uncertainty to the WSI estimates in these regions. In addition, the reuse of wastewater (~1% of

global total water withdrawal) would increase water availability, particularly in Asia (Jones *et al* 2021, van Vliet *et al* 2021).

In this study, and most water scarcity assessments, surface water availability is determined by natural streamflow. It should be noted that surface water availability can be reallocated by human activities, such as reservoir regulations. Thus, the calculation of water availability without considering reservoir regulations may affect the WSI estimates. However, at present, it is difficult to obtain accurate estimates of water availability from regulated streamflow because data on reservoir operations are generally not accessible in most countries. In the future, an online assessment (similar to that conducted by Wada *et al* 2011), which considers improved reservoir regulations, is necessary to reduce the uncertainty in water availability quantification.

5. Conclusions

In this study, we examined the differences in the EFRs estimated by several commonly used methods and quantified the effects of the inclusion of EFRs on global surface water scarcity. We used the FDC-based (Q50 and Q90), Smakhtin, Tennant, Tessmann, VMF, and Q90/Q50 methods. The results suggested large discrepancies in the EFRs estimated using the different methods. We found that the inclusion of EFRs led to significantly different spatial and temporal patterns of water scarcity. The global mean EFRs ranged from $96 \text{ m}^3 \text{ s}^{-1}$ to $428 \text{ m}^3 \text{ s}^{-1}$, and the WSIs calculated using different EFRs indicated that the area experiencing water scarcity ($\text{WSI} > 1$) could vary from 8% (VMF) to more than 52% (Q50) of the global land areas, while the population experiencing water scarcity could be underestimated by 28% (Tennant) to 60% (Q50) of the global total. The areas experiencing water scarcity indicated by the WSIs calculated using the MAF/MMF-based and FDC-based EFRs increased in many basins compared to those calculated without considering EFRs. Moreover, the increments of the areas calculated using the FDC-based (MAF/MMF-based) EFRs increase (decrease) with the AI of the basins. Overall, we deduced that the representation of seasonality in hydrological regimes is essential for producing appropriate EFRs in water scarcity assessment. Thus, in this study, we underscored considerable discrepancies in global surface water scarcity assessments caused by different EFR methods.

However, a comprehensive and appropriate assessment of surface water scarcity considering EFRs remains a challenge to date. The uncertainty in EFR estimates is one of the major underlying factors that limit surface water scarcity assessment and hydrological modeling. By addressing the discrepancies in EFR estimates from different methods, this study aims to improve surface water scarcity assessment and

has instrumental value for water resource management concerning competing water demands between humans and the environment. We call for more attention to the reconciliation of EFRs estimated by different methods for more reasonable global water scarcity assessments.

Data availability statement

The data that support the findings of this study are openly available at the following URL/DOI: <https://doi.org/10.5281/zenodo.4746379>.

Acknowledgments

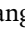
This study was supported by the National Natural Science Foundation of China (41877164), the Swiss National Science Foundation (200021_188686), the National Key R&D Program of China (No. 2019YFA0606903), and the National Natural Science Foundation of China (41625001). W L was supported by the Chinese Universities Scientific Fund (2021RC016). We thank the Inter-Sectoral Impact Model Intercomparison Project (ISIMIP, www.isimip.org) coordination team for providing the ISIMIP2a dataset. The water withdrawal data are publicly available from <https://doi.org/10.5281/zenodo.897933>.

ORCID iDs

Xingcai Liu  <https://orcid.org/0000-0001-5726-7353>

Wenfeng Liu  <https://orcid.org/0000-0002-8699-3677>

Liu Liu  <https://orcid.org/0000-0002-4915-206X>

Qihong Tang  <https://orcid.org/0000-0002-0886-6699>

References

- Acreman M C and Arthington A H 2018 Environmental flows: overview *The Wetland Book: I. Structure and Function, Management, and Methods* ed C M Finlayson, M Everard, K Irvine, R J McInnes, B A Middleton, A A van Dam and N C Davidson (Dordrecht: Springer Netherlands) pp 1813–23
- Acuña V et al 2020 Accounting for flow intermittency in environmental flows design *J. Appl. Ecol.* **57** 742–53
- Alcamo J, Döll P, Henrichs T, Kaspar F, Lehner B, Rösch T and Siebert S 2003 Global estimates of water withdrawals and availability under current and future “business-as-usual” conditions *Hydrol. Sci. J.* **48** 339–48
- Armstrong J D and Nislow K H 2012 Modelling approaches for relating effects of change in river flow to populations of Atlantic salmon and brown trout *Fish. Manage. Ecol.* **19** 527–36
- Arthington A H, Bunn S E, Poff N L and Naiman R J 2006 The challenge of providing environmental flow rules to sustain river ecosystems *Ecol. Appl.* **16** 1311–8
- Belmar O, Velasco J and Martinez-Capel F 2011 Hydrological classification of natural flow regimes to support environmental flow assessments in intensively regulated mediterranean rivers, Segura River Basin (Spain) *Environ. Manage.* **47** 992
- Biemans H, Haddeland I, Kabat P, Ludwig F, Hutjes R W A, Heinke J, Von Bloh W and Gerten D 2011 Impact of reservoirs on river discharge and irrigation water supply during the 20th century *Water Resour. Res.* **47** W03509
- Bondeau A et al 2007 Modelling the role of agriculture for the 20th century global terrestrial carbon balance *Glob. Change Biol.* **13** 679–706
- Campisano A et al 2017 Urban rainwater harvesting systems: research, implementation and future perspectives *Water Res.* **115** 195–209
- Cuthbert M O et al 2019b Observed controls on resilience of groundwater to climate variability in sub-Saharan Africa *Nature* **572** 230–4
- Cuthbert M O, Gleeson T, Moosdorf N, Befus K M, Schneider A, Hartmann J and Lehner B 2019a Global patterns and dynamics of climate–groundwater interactions *Nat. Clim. Change* **9** 137–41
- Döll P, Fiedler K and Zhang J 2009 Global-scale analysis of river flow alterations due to water withdrawals and reservoirs *Hydrol. Earth Syst. Sci.* **13** 2413–32
- Döll P and Lehner B 2002 Validation of a new global 30-min drainage direction map *J. Hydrol.* **258** 214–31
- El-Jabi N and Caissie D 2019 Characterization of natural and environmental flows in New Brunswick, Canada *River Res. Appl.* **35** 14–24
- FAO 2019 Incorporating environmental flows into “water stress” indicator 6.4.2: guidelines for a minimum standard method for global reporting (report) (Rome) p 32 (Available at: <http://www.fao.org/documents/card/en/c/ca3097en/> (Accessed 25 September 2021))
- Gerten D, Hoff H, Rockström J, Jägermeyr J, Kummu M and Pastor A V 2013 Towards a revised planetary boundary for consumptive freshwater use: role of environmental flow requirements *Curr. Opin. Environ. Sustain.* **5** 551–8
- Ghiggi G, Humphrey V, Seneviratne S I and Gudmundsson L 2019 GRUN: an observation-based global gridded runoff dataset from 1902 to 2014 *Earth Syst. Sci. Data* **11** 1655–74
- Gopal B 2013 Methodologies for the assessment of environmental flows *Environmental Flows an Introduction for Water Resources Managers* (New Delhi: National Institute of Ecology) pp 129–82
- Gopal B, Lemons J, Victor R and Schaffer D (eds) 2003 Aquatic biodiversity in arid and semi-arid zones of Asia and water management *Conserving Biodiversity in Arid Regions* 1st edn (Boston, MA: Springer) p 497
- Gosling S et al 2017 ISIMIP2a Simulation Data from Water (global) Sector (GFZ Data Services)
- Grantham T, Zimmerman J, Carah J and Howard J 2019 Stream flow modeling tools inform environmental water policy in California *Calif. Agric.* **73** 33–39
- Grill G et al 2019 Mapping the world’s free-flowing rivers *Nature* **569** 215–21
- Gude V G 2017 Desalination and water reuse to address global water scarcity *Rev. Environ. Sci. Biotechnol.* **16** 591–609
- Hanasaki N et al 2013 A global water scarcity assessment under shared socio-economic pathways—part 2: water availability and scarcity *Hydrol. Earth Syst. Sci.* **17** 2393–413
- Hanasaki N, Kanae S, Oki T, Masuda K, Motoya K, Shirakawa N, Shen Y and Tanaka K 2008 An integrated model for the assessment of global water resources—part 1: model description and input meteorological forcing *Hydrol. Earth Syst. Sci.* **12** 1007–25
- Hanasaki N, Yoshikawa S, Kakinuma K and Kanae S 2016 A seawater desalination scheme for global hydrological models *Hydrol. Earth Syst. Sci.* **20** 4143–57
- Hanasaki N, Yoshikawa S, Pokhrel Y and Kanae S 2018 A quantitative investigation of the thresholds for two conventional water scarcity indicators using a state-of-the-art global hydrological model with human activities *Water Resour. Res.* **54** 8279–94

- Hoekstra A Y and Mekonnen M M 2012 The water footprint of humanity *Proc. Natl Acad. Sci.* **109** 3232–7
- Hoekstra A Y, Mekonnen M M, Chapagain A K, Mathews R E, Richter B D and Añel J A 2012 Global monthly water scarcity: blue water footprints versus blue water availability *PLoS One* **7** e32688
- Huang Z et al 2018 Reconstruction of global gridded monthly sectoral water withdrawals for 1971–2010 and analysis of their spatiotemporal patterns *Hydrol. Earth Syst. Sci.* **22** 2117–33
- Jägermeyr J, Pastor A, Biemans H and Gerten D 2017 Reconciling irrigated food production with environmental flows for sustainable development goals implementation *Nat. Commun.* **8** 1–9
- Jeliaskov A et al 2020 A global database for metacommunity ecology, integrating species, traits, environment and space *Sci. Data* **7** 6
- Jones E R, van Vliet M T H, Qadir M and Bierkens M F P 2021 Country-level and gridded estimates of wastewater production, collection, treatment and reuse *Earth Syst. Sci. Data* **13** 237–54
- Liu J, Liu Q and Yang H 2016a Assessing water scarcity by simultaneously considering environmental flow requirements, water quantity, and water quality *Ecol. Indic.* **60** 434–41
- Liu X 2021 *Global environmental flow requirement estimates based on multimodel simulations [Data set]* Zenodo (<https://doi.org/10.5281/ZENODO.4746379>) (Accessed 25 September 2021)
- Liu X, Tang Q, Cui H, Mu M, Gerten D, Gosling S, Masaki Y, Satoh Y and Wada Y 2017 Multimodel uncertainty changes in simulated river flows induced by human impact parameterizations *Environ. Res. Lett.* **12** 025009
- Liu X, Tang Q, Liu W, Veldkamp T I E, Boulange J, Liu J, Wada Y, Huang Z and Yang H 2019 A spatially explicit assessment of growing water stress in China from the past to the future *Earth's Future* **7** 1027–43
- Liu X, Tang Q, Zhang X and Leng G 2016b Modeling the role of vegetation in hydrological responses to climate change *Terrestrial Water Cycle and Climate Change: Natural and Human-Induced Impacts* (Washington, DC: American Geophysical Union) pp 193–208
- Lo A G and Gould J 2015 *Rainwater harvesting: global overview Rainwater Harvesting for Agriculture and Water Supply* ed Q Zhu, J Gould, Y Li and C Ma (Berlin: Springer) pp 213–33
- Mekonnen M M and Hoekstra A Y 2020 Blue water footprint linked to national consumption and international trade is unsustainable *Nat. Food* **1** 792–800
- Müller Schmied H, Eisner S, Franz D, Wattenbach M, Portmann F T, Flörke M and Döll P 2014 Sensitivity of simulated global-scale freshwater fluxes and storages to input data, hydrological model structure, human water use and calibration *Hydrol. Earth Syst. Sci.* **18** 3511–38
- Okil T 2006 Global hydrological cycles and world water resources *Science* **313** 1068–72
- Pastor A V, Ludwig F, Biemans H, Hoff H and Kabat P 2014 Accounting for environmental flow requirements in global water assessments *Hydrol. Earth Syst. Sci.* **18** 5041–59
- Pastor A V, Palazzo A, Havlik P, Biemans H, Wada Y, Obersteiner M, Kabat P and Ludwig F 2019 The global nexus of food–trade–water sustaining environmental flows by 2050 *Nat. Sustain.* **2** 499–507
- Poff N L et al 2010 The ecological limits of hydrologic alteration (ELOHA): a new framework for developing regional environmental flow standards *Freshw. Biol.* **55** 147–70
- Richter B D 2010 Re-thinking environmental flows: from allocations and reserves to sustainability boundaries *River Res. Appl.* **26** 1052–63
- Richter B D, Baumgartner J V, Powell J and Braun D P 1996 A method for assessing hydrologic alteration within ecosystems *Conserv. Biol.* **10** 1163–74
- Richter B D, Baumgartner J, Wigington R and Braun D 1997 How much water does a river need? *Freshw. Biol.* **37** 231–49
- Sayre R et al 2014 *A new map of global ecological land units—An ecophysiological stratification approach* (Washington, D.C.: Association of American Geographers) p 46
- Schewe J et al 2014 Multimodel assessment of water scarcity under climate change *Proc. Natl Acad. Sci. USA* **111** 3245–50
- Sheffield J, Goteti G and Wood E F 2006 Development of a 50-year high-resolution global dataset of meteorological forcings for land surface modeling *J. Clim.* **19** 3088–111
- Smakhtin V U, Revenga C and Döll P 2004 A pilot global assessment of environmental water requirements and scarcity *Water Int.* **29** 307–17
- Sood A et al 2017 Global environmental flow information for the sustainable development goals (International Water Management Institute (IWMI)) (<https://doi.org/10.5337/2017.201>)
- Tang Q, Okil T, Kanae S and Hu H 2008 Hydrological cycles change in the Yellow River Basin during the last half of the twentieth century *J. Clim.* **21** 1790–806
- Taylor R G et al 2013 Ground water and climate change *Nat. Clim. Change* **3** 322–9
- Tennant D L 1976 Instream flow regimens for fish, wildlife, recreation and related environmental resources *Fisheries* **1** 6–10
- Tessmann S A 1980 *Environmental Assessment, Technical Appendix E in Environmental Use Sector Reconnaissance Elements of the Western Dakotas Region of South Dakota Study* (Brookings, SD: Water Resources Research Institute, South Dakota State University)
- Theodoropoulos C, Georgalas S, Mamassis N, Stamou A, Rutschmann P and Skoulikidis N 2018 Comparing environmental flow scenarios from hydrological methods, legislation guidelines, and hydrodynamic habitat models downstream of the Marathon Dam (Attica, Greece) *Ecology* **11** e2019
- Trabucco A and Zomer R J 2019 Global aridity index and potential evapotranspiration (ET0) climate database v2 (CGIAR Consortium for Spatial Information (CGIAR-CSI)) (Available at: <https://doi.org/10.6084/m9.figshare.7504448.v3>) (Accessed 25 September 2021))
- USFWS 1981 *Standards for the Development of Habitat Suitability Index Models* (Washington, D.C.: Division of Ecological Services, US Fish and Wildlife Service)
- van Vliet M T H, Jones E R, Flörke M, Franssen W H P, Hanasaki N, Wada Y and Yearsley J R 2021 Global water scarcity including surface water quality and expansions of clean water technologies *Environ. Res. Lett.* **16** 024020
- Wada Y et al 2016 Modeling global water use for the 21st century: the water futures and solutions (WfS) initiative and its approaches *Geosci. Model Dev.* **9** 175–222
- Wada Y, Beek L P H, van Kempen C M, van Reckman J W T M, Vasak S and Bierkens M F P 2010 Global depletion of groundwater resources *Geophys. Res. Lett.* **37** L20402
- Wada Y, van Beek L P H, Viviroli D, Dürr H H, Weingartner R and Bierkens M F P 2011 Global monthly water stress: 2. Water demand and severity of water stress *Water Resour. Res.* **47** W07518
- Wada Y, Wissler D and Bierkens M F P 2014 Global modeling of withdrawal, allocation and consumptive use of surface water and groundwater resources *Earth Syst. Dyn.* **5** 15–40
- Weedon G P, Balsamo G, Bellouin N, Gomes S, Best M J and Viterbo P 2014 The WFDEI meteorological forcing data set: WATCH forcing data methodology applied to ERA-Interim reanalysis data *Water Resour. Res.* **50** 7505–14
- Zhao F et al 2017 The critical role of the routing scheme in simulating peak river discharge in global hydrological models *Environ. Res. Lett.* **12** 075003